The effect of ambient atmosphere in the annealing of indium tin oxide films

A. J. Steckl and G. Mohammed[a)]
Rensselaer Polytechnic Institute, Electrical and Systems Engineering Department, Troy, New York 12181

(Received 17 September 1979; accepted for publication 13 March 1980)

Isochronal annealing experiments on dc-sputtered indium tin oxide (ITO) films in inert (N_2), reducing (N_2/H_2) and oxidizing atmospheres were cumulatively performed over the 50→500→50 °C range. Three anneal regimes have been identified. In region I, T_A = 50→200 °C, crystallization occurs, resulting in a sharp drop in sheet resistance (R_s) due to increasing mobility. $T_A \simeq 200$ °C results in a minimum R_s. In region II, 200→500→200 °C, R_s is proportional to T_A, increasing (decreasing) during the forward (reverse) anneal cycle. This behavior is apparently due to a temperature-dependent active oxygen concentration and its effect on the carrier concentration. In region III, 200→50 °C, R_s is constant with T_A. Optical transmission and x-ray diffraction experiments were performed at 100 °C intervals. Successive anneals tended to increase the transmission in the visible and near-UV regions and to decrease it in the near- and far-IR region. Strong evidence of the Burstein-Moss shift was observed and an extrapolated intrinsic band gap of 3.85 eV was determined. Free-carrier absorption over the 2–5-μm regions was evident after the 200 °C anneal for all ambients. From the x-ray data, no evidence of crystallinity was observed in the as-deposited case and for anneals up to 100 °C. For anneals in the 300–500 °C range, a grain size of the order of 600 Å with an orientation normal to the (222) plane was observed for all ambients.

PACS numbers: 81.40.Tv, 81.40.Rs, 61.55.Hg

I. INTRODUCTION

Indium Tin Oxide (ITO) films have found many applications in a variety of electro-optical devices which need transparent electrodes. The effect of heat treatment on the electrical and optical properties of ITO films is well-known.[1-5] To date, annealing experiments reported have used a combination of temperature and choice of ambient such that a minimum sheet resistance and maximum visible transmission be obtained. Consequently, the exact role of the ambient atmosphere in the annealing process could not be unambiguously ascertained. It was, therefore, the goal of this work to investigate the effect of the ambient on the resulting electrical, optical, and structural properties of annealed ITO films. Three ambient atmospheres were chosen: (a) an inert ambient, N_2 gas; (b) a reducing ambient, $(85/15)N_2/H_2$; (c) an oxidizing ambient, air.

ITO films were dc sputtered in an Ar partial pressure on freshly cleaved BaF_2 substrates from a Sn/In target of 10/90 ratio. The film thickness was 1000 ± 50 Å. Isochronal anneals of 60 min were cumulatively performed in an electrical resistance furnace over the 50→500→50 °C range at 25 °C intervals. The anneal duration of 60 min was chosen based on reported results[3,4,6] which indicate that after 30–40 min no further effects were observed. Six films were used, two for each ambient. After each anneal, the samples were allowed to cool down to room temperature in their respective atmosphere. The as-deposited films had a smoky-brown appearance, typical of metal-rich ITO. The film color gradually disappeared with each consecutive anneal. At 200 °C the films appeared colorless. The film sheet resistance was measured after each anneal using a four-point probe. Using a hot-point probe technique, the film conductivity was verified to be *n* type. The optical transmission was measured at 100 °C intervals on Berkman DK2A (0.3–2.5 μm) and Per-

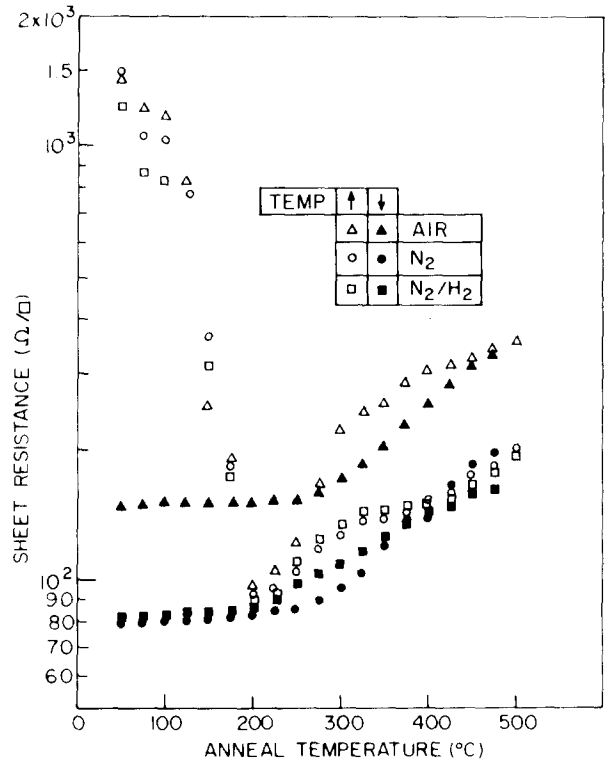

FIG. 1. Sheet resistance for cumulative isochronal (60 min) anneals in different ambients.

[a)]Present address: Harris Corp., Semiconductor Div., Melbourne, Fla.

 0021-8979/80/073890-06$01.10

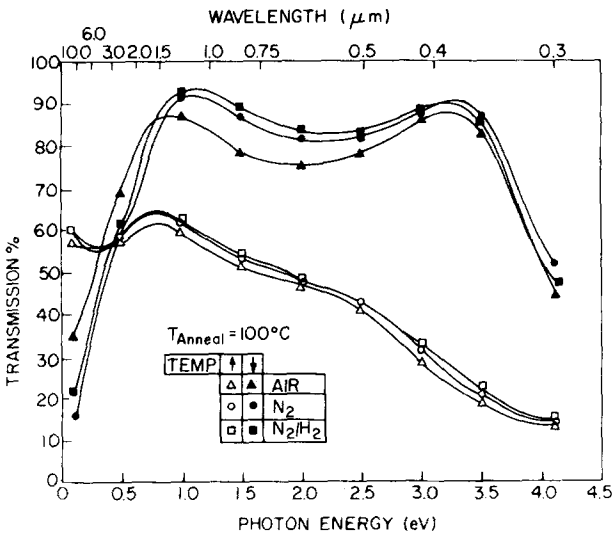

FIG. 2. ITO transmission after the 100 °C anneal (↑ increasing temperature cycle, ↓ decreasing temperature cycle). Symbols for identification only, continuous lines are the actual experimental data.

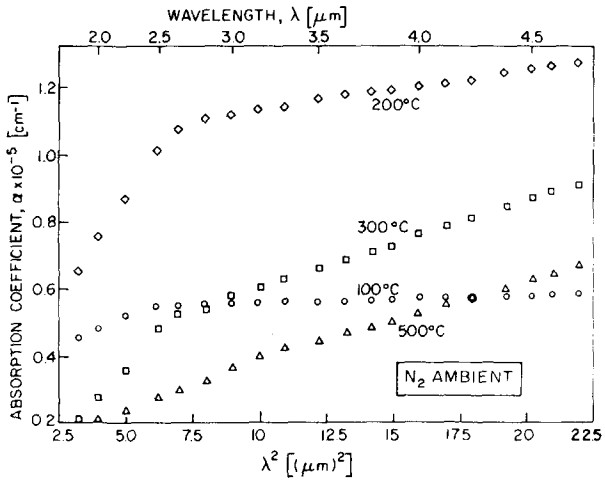

FIG. 4. Absorption coefficient vs wavelength for different anneal temperatures (N_2 ambient).

kin-Elmer (2.5-12 μm) spectrometers. Similarly, x-ray diffraction data was taken on a General Electric XRD-6 diffractrometer at the same 100 °C intervals.

II. SHEET RESISTANCE

The sheet resistance R_s of all ITO films was measured over the entire annealing range of 50→500→50 °C at 25 °C intervals, as shown in Fig. 1. Each point represents the average of a number of readings on the two samples used in each ambient. The R_s of the as-deposited films was too high to be measured with our equipment. The first data points were taken after the 50 °C anneal and they lie in the $1\text{–}2\times10^3$-$\Omega/\square$ range. Successive anneals from 50 to 200 °C resulted in a dramatic drop in R_s for all ambients. After the 200 °C anneal, R_s for all samples was within a 5 $\Omega/\square$ range, from 90 to 95 $\Omega/\square$. The equivalent conductivity is around 1×10^3 $(\Omega\ \text{cm})^{-1}$. Subsequent anneals, up to 500 °C, resulted in moderate but continuous increases in R_s thus revealing that the 200 °C anneal resulted in a minimum in sheet resistance. The increase in R_s between 200 and 500 °C was a factor of ~3.5 for air and ~2.2 for nitrogen and forming gas ambients. At this point, the direction of the temperature cycle was reversed with each subsequent anneal being performed at a temperature 25 °C lower. Over the 500→250 °C range, the R_s was apparently reversible, following roughly the 250→500 °C curve for all ambients. For anneals over the 250→50 °C range, R_s remained constant showing that this part of the process is irreversible. In the case of N_2 and N_2/H_2 ambients, this constant value was slightly less than the minimum achieved at 200 °C in the forward part of the temperature cycle. For the air ambient, the constant R_s over the 250→50 °C range was approximately 50% higher than the previously achieved minimum.

The results of annealing experiments presented above confirm the presence of an R_s minimum for all ambients during the forward part of the cycle. The minimum occurs at

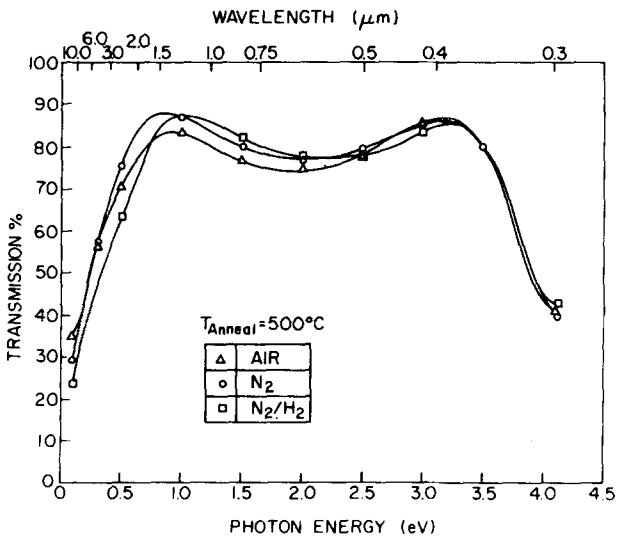

FIG. 3. ITO transmission after the 500 °C anneal.

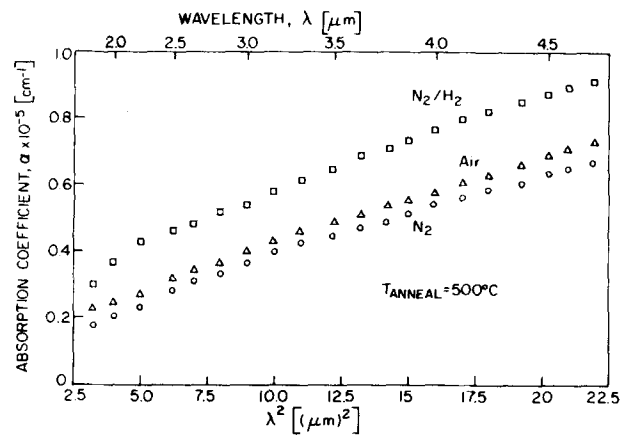

FIG. 5. Absorption coefficient vs wavelength for different ambients.

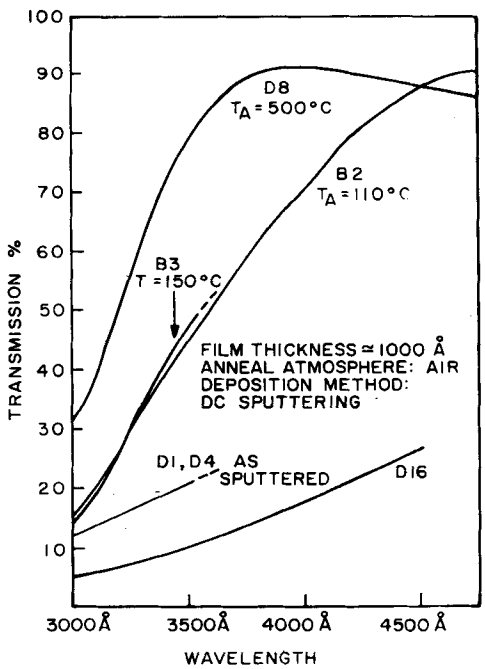

FIG. 6. Near-UV transmittance of ITO films for different anneal conditions.

~200 °C in all cases verifying the previously reported[5] minimum for identical ITO films annealed in air only. These results for our dc sputtered films were not generally observed by Pankratz[6] for reactively sputtered films annealed in similar ambients. Rather, he reported a monotonically decreasing R_s with anneal temperature. However, both Pankratz[6] and Hoffman[7] briefly report that in the case of ITO films reactively sputtered in a high Ar/O_2 partial pressure ratio a minimum does exist at 200 °C for oxygen and forming gas ambients[6] and at 450 °C for air ambient.[7] However, a meaningful comparison with our results is difficult since no annealing time is given.

III. OPTICAL TRANSMISSION

The optical transmission of the ITO films was monitored simultaneously with the sheet resistance, but data was taken only at 100 °C intervals. Figure 2 shows the transmission of the films after the initial and final 100 °C anneal. After the initial 100 °C anneal, only very weak evidence of the energy band gap is observed. In Fig. 3, the transmission measured after the 500 °C anneal is shown. The absorption edge is clearly evident for all ambients in the 3.2–4.0-eV range. As can be seen by comparing the data in Fig. 3 with the transmission present after the final 100 °C anneal (Fig. 2), anneals in the reverse cycle, 500→100 °C, have little effect on the general characteristic of the transmission. In general, the choice of ambient did not significantly affect the general shape of the transmission spectrum of ITO for any of the temperatures used in our annealing experiments.

The absorption effect of free carriers generated during the anneal cycle was investigated in some detail. The classical formula for the free-carrier absorption coefficient[8] is given by

$$\alpha_f = Nq^2\lambda^2/m^*8\pi^2nc^3\tau, \quad (1)$$

where N is the carrier concentration, n is the index of refraction, τ is the carrier relaxation time, m^* is the effective mass, and c is the speed of light. This formula predicts the square-law dependence of α_f on the wavelength normally seen in the infrared region. In Fig. 4, we have plotted the absorption coefficient obtained from our optical transmission data for N_2-annealed films versus λ^2 over the 2–4.75-μm region. The films annealed at 100 °C exhibit no wavelength dependence and thus do not have a carrier concentration sufficient to result in significant free-carrier absorption. After the 200 °C anneal, a linear relation between α_f and λ^2 is obtained over the 2.5–4.75-μm range. The same linear relation is observed for the 300 and 500 °C data. While the same general effect of free-carrier absorption is observed for all annealing ambients, as shown in Fig. 5, the absorption coefficient for N_2/H_2 anneals is somewhat larger than for the other two ambients.

The near-UV transmittance for ITO films annealed in air is shown in Fig. 6. A shift in absorption edge to shorter wavelengths is evident as the anneal temperature is increased. As discussed below (see Sec. V) this shift in absorption edge with anneal temperature is related to the increasing carrier concentration which results in a higher optical gap.

IV. FILM STRUCTURE

In general, with the exception of color, the visual appearance of the ITO films did not change during the anneal cycle. At a magnification of 20KX, under the scanning electron microscope (SEM), the smooth appearance of as-deposited films was still present after the 500 °C anneal in air. In the case of N_2/H_2 ambient, metal precipitates were observed under the SEM after the 500 °C anneal. As shown in the microphotograph in Fig. 7, the radius of the precipitates varies between ~0.1 and 0.5 μm.

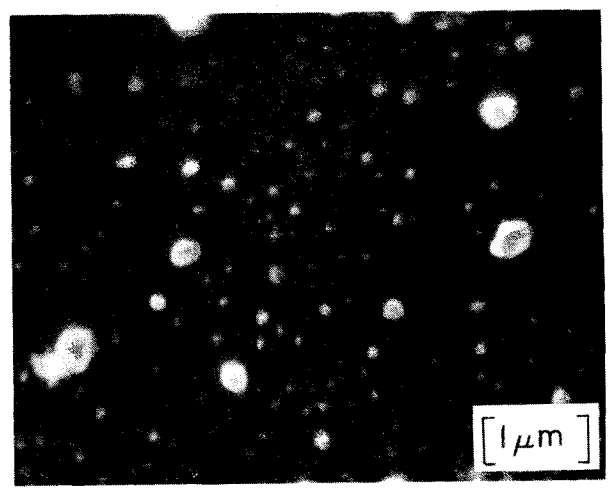

FIG. 7. SEM microphotograph of ITO film after the 500 °C anneal in forming gas. Magnification is 20KX.

TABLE I. X-ray diffraction data for ITO films annealed at 500 °C.

	D1[a]			D2[a]			D3[b]			D4[b]			D5[c]			D6[c]	
2θ	I[d]	I/I_1[e] (%)	Grain size (Å)	I	I/I_1 (%)	Grain size (Å)	I	I/I_1 (%)	Grain size (Å)	I	I/I_1 (%)	Grain size (Å)	I	I/I_1 (%)	Grain size (Å)	I	I/I_1 (%)	Grain size (Å)
25° (A)	24	100		23	100		20	100		25	100		18	100		20	100	
31° (B)	18	75	634	16	70	610	10	50	532	14	55	568	14	77	687	13	65	634
51° (A)	14	58		15	65		10	50		13	52		11	61		10	50	
80° (A)	16	68		15	65		11	55		15	60		12	66		15	75	

[a]Annealed in air.
[b]Annealed in nitrogen.
[c]Annealed in forming gas.
[d]I = Intensity.
[e]I_1 = Intensity of strongest peak.
(A) BaF_2 peaks.
(B) In_2O_3 peaks.

X-ray diffraction measurements were also performed on the as-deposited films and at 100 °C intervals in the anneal cycle. Diffraction data taken after the 500 °C anneal is shown in Table I. The major peak observed was at an angle $2\theta = 25°$ and corresponds to BaF_2 with a preferred orientation normal to the (111) plane, as verified by ASTM powder diffraction data. The peaks at 51° and 80° are minor BaF_2 components. The peak at 31° was verified to correspond to In_2O_3 with a preferred orientation normal to the (222) plane. The grain size was determined from the diffraction line broadening using the Scherrer equation[9]

$$D = K\lambda / \beta \cos\theta , \tag{2}$$

where θ is the diffraction angle, λ is the average wavelength of the Cu K_α radiation (1.54 Å), and K is the shape factor with a value of 0.9. β is the line broadening

$$\beta = B - b , \tag{3}$$

where B is the In_2O_3 full width diffraction line at one-half maximum intensity (FWHM) and b is the effect of the instrument as determined from the broadening of the monocrystalline silicon diffraction line. A grain size of 580–690 Å is calculated for the three sets of samples. Due to an instrument broadening error of $\pm$ 30%, the uncertainty in the measurements is of the order of $\pm$ 50%, and thus the effect of different ambients cannot be extracted. However, it is clear that preferred ITO growth has taken place on the BaF_2 substrate. Data obtained on the grain size after anneals at various temperatures is shown in Table II. For the as-deposited films, as well as after the 100 °C anneal, no In_2O_3 peak is detected. After the 200 °C anneal is very small peak is detected at $2\theta = 31°$, but no grain size could be determined due to the predominant background noise. For anneals in the 300–500 °C range, the grain size shows the same slight increase with temperature for all ambients indicating again no strong effect on the part of the annealing atmosphere.

The same (222) orientation was reported for rf-sputtered films on the (111) face of CaF_2 (Ref. 2). While these films received no postdeposition treatment, the estimated substrate temperature during deposition was between 700–800 °C. The grain size that we have measured, ~600 Å, is somewhat larger than values previously reported. For example, Thornton and Hedgcoth[3] have reported a grain size of 300 Å for dc reactively sputtered ITO films after a 400 °C anneal.

V. DISCUSSION AND CONCLUSIONS

The effect of anneal temperature T_A on the sheet resistance of the ITO films can be separated into three regions. In region I, 50→200 °C, increasing T_A results in a sharp drop in R_s. At the same time the x-ray diffraction data indicates that the first evidence of observable grain size is detected after the

TABLE II. X-ray diffraction data for In_2O_3 peak ($2\theta = 31°$) for different anneal temperatures.

	D1[a]			D2[a]			D3[b]			D4[b]			D5[c]			D6[c]	
Anneal temp.	I[d]	I/I_1[e] (%)	Grain size (Å)	I	I/I_1 (%)	Grain size (Å)	I	I/I_1 (%)	Grain size (Å)	I	I/I_1 (%)	Grain size (Å)	I	I/I_1 (%)	Grain size (Å)	I	I/I_1 (%)	Grain size (Å)
200° C	5	20	**	8	24	**	4	22	**	6	32	**	5	25	**	6	21	**
300° C	18	54	560	11	36	**	8	44	**	10	45	458	9	50	550	11	55	568
400° C	21	62	588	14	48	485	10	49	485	12	48	485	12	63	589	12	60	580
500° C	18	75	634	16	70	610	10	50	532	14	55	568	14	77	687	13	65	634

[a]Annealed in air.
[b]Annealed in nitrogen.
[c]Annealed in forming gas.
[d]I = Intensity at In_2O_3 Peak, $2\theta = 31°$.
[e]I_1 = Intensity of strongest peak.
**Peak is present but grain size could not be measured due to background noise.

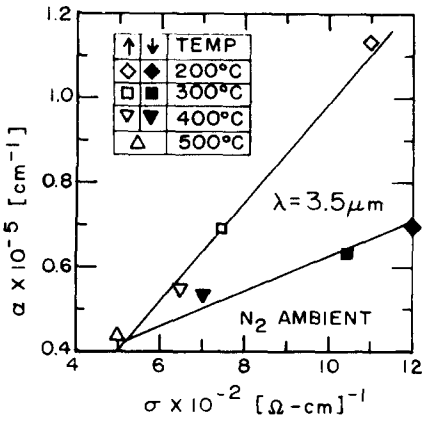

FIG. 8. Absorption coefficient at 3.5 μm vs ITO film conductivity for region II anneals in N_2.

200 °C anneal. We can therefore ascribe the effects observed in region I to a rapid increase in mobility accompanying the process of crystallization. $T_A \simeq 200$ °C appears to be the transition point between amorphous and polycrystalline films. Region II covers approximately the range 200→500→200 °C, wherein R_s is roughly reversible, increasing during the forward part of the anneal cycle and decreasing during the reverse part of the cycle. The behavior of R_s in region II can be generally, but not completely, explained on the basis of electron trapping by excess oxygen.[10] Since the grain size measured for $T_A > 300$ °C increases only slightly, one can assume that the mobility is also only slowly increasing with temperature once the film has become polycrystalline. After each anneal, the active oxygen equilibrium concentration achieved for that particular temperature dictates the free-carrier concentration and therefore the conductivity. This conclusion is supported in part by the effect of annealing on the ITO infrared and near-ultraviolet transmission. In Fig. 8, the absorption coefficient at $\lambda = 3.5\,\mu$m is plotted as a function of conductivity for region II anneals in N_2. During the forward part of the cycle, $T_A = 200 \rightarrow 500$ °C, a linear relationship with a slope of 1.2 is observed. In the reverse part of the cycle, $T_A = 500 \rightarrow 200$ °C, again a linear relationship is present, this

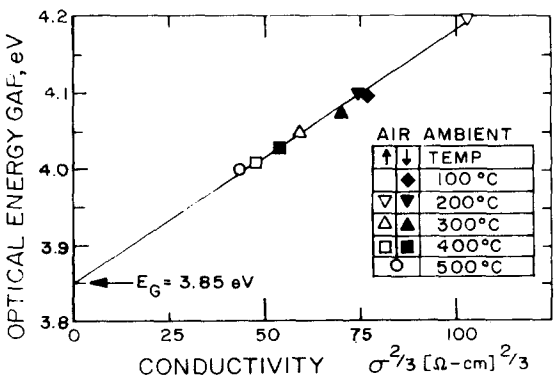

FIG. 9. Optical energy gap vs conductivity for ITO films annealed at various temperatures in air.

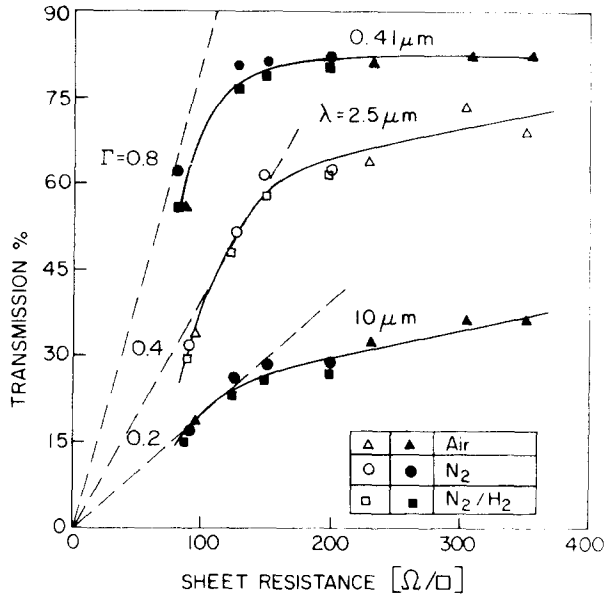

FIG. 10. Relationship between optical transmission and sheet resistance.

time with a slope of 0.4. The fact that the free-carrier absorption coefficient [see Eq. (1)] is directly proportional to the conductivity for both forward and reverse cycles verifies that changes in R_s for this regime are due to the carrier concentration.

In the near-UV, the effect of annealing is to shift the absorption edge to higher energy due to the Burstein effect.[11] The shift is given by

$$\Delta E_B = E_{G,i} - E_{G,\mathrm{opt}} = (h^2/8m^*)(3N/\pi)^{2/3}, \qquad (4)$$

where $E_{G,i}$ is the intrinsic energy gap, $E_{G,\mathrm{opt}}$ is the optical gap, N is the free electron density, and m^* is the electron effective mass. As pointed out by Haynes and Bube,[4] if the mobility is constant, the energy gap shift and therefore the optical gap is proportional to the two-thirds power of the conductivity. In Fig. 9, $E_{G,\mathrm{opt}}$ is plotted as a function of $\sigma^{2/3}$ for ITO films annealed in air at $T_A = 200 \rightarrow 500 \rightarrow 100$ °C. The $E_{G,\mathrm{opt}}$ points were taken at energies for which the transmission was one-half of its maximum value. A linear relationship is observed, indicating once again that the mobility is indeed constant in region II. The data points corresponding to region I do not follow the linear relationship shown in Fig. 9. The extrapolation of the region II date to zero conductivity results in an intrinsic energy gap of $E_{G,i} = 3.85$ eV. This matches closely the value of 3.75 eV obtained by Weiher and Ley[13] for the direct energy gap of In_2O_3 thin films.

Now, if one assumes that after higher-temperature anneals a larger active oxgyen equilibrium concentration is achieved, a lower σ and a higher R_s would result. If a subsequent anneal is performed at a lower temperature, the equilibrium oxgyen concentration is reduced, resulting in a higher σ and therefore a reversible R_s. As expected, the increase in R_s during the forward cycle of region II is most pronounced for anneals performed in air, since in this case a higher equilibrium oxygen concentration should result. However, no substantial difference was observed between

N_2 and N_2/H_2 anneals. This is somewhat unexpected since the forming gas should reduce the oxygen concentration. Similar minimal differences between N_2 and N_2/H_2 anneals was reported by Pankratz[6] for a 90/10 mixture. On the other hand, when ITO films were annealed in pure H_2, as in the data reported by Haynes and Bube,[4] a difference as large as a factor of 2 in resistivity is observed. It is, therefore, very likely that when low H_2 concentration forming gas is used, the reducing effect is negligible compared to the dominating effect of the much larger concentration N_2 gas. Region III covers the range $T_a \approx 200 \rightarrow 50$ °C. In this region R_s is constant with anneal temperature, possibly because the temperature is too low to cause further oxygen diffusion or activation.

Since both the optical transmission and the sheet resistance must be considered when evaluating a material for use as a transparent electrode, a figure of merit normally defined as $\Gamma = (T\,\%)/R_s$ is employed. In Fig. 10, the relationship between transmission and sheet resistance is shown at various wavelengths. The data points included are for anneals in all three ambients at temperatures from 200 to 500 °C. Roughly the same type of characteristics are obtained at visible, near-IR, and far-IR wavelengths. At each wavelength the highest Γ is obtained at the initial part of the curve. These data points are from the 200 °C anneal where a minimum in R_s is obtained, and they represent the optimum annealing conditions. If the films are annealed under these optimum conditions the effect of ambient can be seen to be negligible. While greater transmission can be obtained for $T_A > 200$ °C, the accompanying increase in R_s results in a decreasing Γ.

[1]D. B. Fraser and H. D. Cook, J. Electrochem. Soc. **119**, 1368 (1972).
[2]J. C. C. Fan and F. J. Bachner, J. Electrochem. Soc. **122**, 1719 (1975).
[3]J. A. Thornton and V. L. Hedgcoth, J. Vac. Sci. Technol. **13**, 117 (1976).
[4]W. G. Haines and R. H. Bube, J. Appl. Phys. **49**, 304 (1978).
[5]A. J. Steckl, Infrared Phys. **16**, 145 (1976).
[6]J. M. Pankratz, J. Electron. Mater. **1**, 95 (1972).
[7]V. Hoffman, Optical Spectra, November, 60 (1978).
[8]J. L. Pankove, *Optical Processes in Semiconductors* (Dover, New York, 1971).
[9]H. P. Klug and L. E. Alexander, *X-ray Diffraction Procedure for Polycrystalline and Amorphous Materials* (Wiley, New York, 1954).
[10]H. Hoffman, A. Dietrich, J. Pickl, and D. Krause, Appl. Phys. **16**, 381 (1978).
[11]E. Burstein, Phys. Rev. **93**, 632 (1954).
[12]H. Kostlin, R. Jost, and W. Lenis, Phys. Status Solidi A **29**, 87 (1975).
[13]R. L. Weiher and R. P. Ley, J. Appl. Phys. **37**, 299 (1966).